Fachtagung "Lasermethoden in der Strömungsmesstechnik"
9. – 11. September 2014, Karlsruhe

CHARACTERIESIRUNG DER PARTIKELBEWEGUNG AUF REGELMÄSIG ANGEORDNETEN SUBSTRATEN IN EINER LAMINAREN SCHERSTRÖMUNG

CHARACTERIZATION OF SHEAR INDUCED GRANULAR MOTION ON REGULAR SUBSTRATES UNDER LAMINAR CONDITIONS

J.R. Agudo[1,2], J. Park[1], J. Lee[1], A. Wierschem[2]

[1]Institute of Fluid Mechanics, FAU Busan Campus, University of Erlangen-Nuremberg,
618-230 Busan, Republic of Korea
[2]Institute of Fluid Mechanics, University of Erlangen-Nuremberg,
D-91058 Erlangen, Germany

Granulare Medien, Partikel- und Sedimenttransport, Strömungsfeld
Granular systems, particle and sediment transport, flow field

Abstract

We study experimentally the critical conditions for incipient motion of spherical particles deposited on a regular substrate under laminar flow conditions. The substrates are in triangular and quadratic arrangements of identical glass spheres of same size. The free particles are submitted to a laminar flow with a triangular velocity profile induced by the parallel-disk configuration of a MCR 301 rotational rheometer. The particle motion is simultaneously recorded from the top view through the transparent rotating disk, and from the lateral view through the Plexiglas walls of the container placed in the rheometer. For the first case, we use a digital camera with a chip of 752 x 480 pixels and a frame rate up to 120 Hz coupled to a macro objective that incorporates a tilted mirror. For the latter, a 1280x1024 pixels digital camera together with a 180mm f/3.5 macro lens is used. In order to determine the particle mean velocity, we developed an image processing algorithm which optically tracks and evaluates the bead position on the substrate.
We found that for particle Reynolds numbers of order one and smaller, the critical Shields number is independent from the particle density and from the particle Reynolds numbers, but it depends significantly on the geometry of the substrate. In addition, we studied how neighboring beads affect the onset of motion. We observed that, in stream-wise direction, only spheres that are closer than about 3 particle diameters influence incipient motion by shielding to the shear flow. Besides incipient motion, we also study the particle motion along the substrate at supercritical Shields numbers and show how the substrate geometry also affects the mean velocity of the particle. The velocity appears to be a linear function of the supercritical Shields number for all the substrates. However, the slope of the curve as well as the x-intercept strongly depend on the substrate geometry. Taking data for different viscosities, particle densities and substrate geometries into account and based on ideas of Bagnold and Charru et al., we obtained a master curve between the particle velocity normalized by the Stokes settling velocity and the super critical Shields number.

Introduction

Shear induced granular motion has many important applications in natural and industrial processes. Environmental examples include sediment transport in river and oceans, bed erosion or dune formation (Groh et al. 2008). On the other hand, pneumatic conveying or cleaning of surfaces, are basic operations in food and pharmaceutical industries.
Despite most of the studies in this field are addressed by turbulent flows over disordered heterogeneous beds (Shields 1936, Dey and Papanicolau 2008, Wierschem et al. 2008, 2009), several authors have recently focused on the bed-load transport under laminar conditions (Charru et al. 2004, 2007, Loiseleux et al. 2005, Lobkovsky et al., Ouriemi 2007, J.J. Derksen 2010). Charru et al., for instance, presented an erosion-deposition model, which could be also extended to turbulent flows, and was able to describe the transport of particles with a heterogeneous particle size (Charru et al. 2004).
Indeed, granular motion under laminar conditions is directly related to some natural processes, as in final stage of outburst floods (Carrivick et al.), and industrial applications as heavy oil production, gas-hydrate generation and transport in pipelines or microfluidics (Sawetzki et al. 2008, Thompson et al. 2010). Here, the number of well controlled systems, including regular structured beds, has increased a lot over the last years. Internal mechanisms taking place in filtration process also involve regular patterns and low Reynolds number. On the other hand, recent studies show how the stone organization of the bed is also critical to avoid clogging in horizontal subsurface-flow treatment wetlands (Pozo-Morales et. al).
In previous studies, we quantified the strong effect of the bed arrangement on the onset of motion of a single particle (Agudo and Wierschem 2012). We later showed how additional neighboring particles affected the incipient motion, observing values of the critical Shields number for the onset of motion in good agreement to previous erosion-deposition models for disordered beds (Agudo et. al 2014). In addition, we described the different mechanism of motion taking place on it. Besides the incipient particle motion, we study here the influence of the bed geometry on the particle mean velocity during its displacement along regular substrates.

Experimental set-up

Mobile beads of equal size of around 400 μm but different materials are placed on regular substrates. They consist of a monolayer of soda-lime glass spheres of same size, fixed and arranged according to triangular and quadratic configurations (see Figures 1c and 1d). For the latter, we use two substrates with different spacing between particles. The substrates, with dimensions of 70x15 mm, are glued to glass microscope slides of 70x25 mm and placed off-centered on the bottom of a transparent Plexiglas box which dimensions are illustrated in Figure 1a. This container is placed in an MCR 301 rotational rheometer from Anton Paar (Figure 1b) and filled with two different silicon oils. The parallel-disk configuration induces a laminar flow with a triangular velocity profile. The gap width, h, is defined as the distance from the top of the substrate spheres to the rotating plate (see Figure 1e), and the angular frequency, Ω, are parameters controlled with the rheometer.
All experiments are performed at a gap width of 2 mm. Different fluids and particle materials permit us to vary the relative density difference between the particle and the liquid, $\rho_s/\rho - 1$, , where ρ_s and ρ are particle and liquid densities, respectively, as well as the particle Reynolds number, Re_P, which remains below 1 for all experiments. Reynolds number, Re, and particle Reynolds number are defined as:

$$Re = \frac{\Omega r h}{\nu} \quad , \quad Re_P = Re \left(\frac{D_P}{h}\right)^2 \tag{1}$$

where ν is the kinematic viscosity and D_P is the particle diameter.

For our setup, the Shields number, which compares the characteristic shear stress acting on the particle to the resistant specific particle weight that retains it in place, is given by:

$$\theta = \frac{\nu \Omega r}{\left(\rho_s/\rho - 1\right) h g D_P} \tag{2}$$

Table 1 summarizes the particle and fluid properties. The operating temperature is fixed at (295.16 ± 0.5) K and controlled with a P-PTD 200 Peltier element connected to the rheometer. The mobile beads are situated at a radial distance of 50 mm from the turning axis and at a distance of about 35 mm from the substrate's upstream edge, i.e. in line with the rotating disk symmetrical axis.
We apply a sudden shear-rate jump with a step width of about 0.02 s over the mobile beads, starting from subcritical conditions to a certain supercritical Shields numbers that is kept constant while the particle moves along the substrate. Particle motion is then simultaneously recorded from the top view through the transparent rotating disk (Figure 1a), and from the lateral view through the Plexiglas container walls (Figure 1b). For the first case, we use a digital camera with a chip of 752 x 480 pixels and a frame rate up to 120 Hz coupled to a macro objective that incorporates a tilted mirror. For the latter, a 1280x1024 pixels digital camera together with a 180mm f/3.5 macro lens is used. In order to determine the particle mean velocity, we developed an image processing algorithm, which optically tracks and evaluates the bead position on the substrate.

Table 1: Resume of particle and liquid properties

Particle material	Density ρ_s [g cm^{-3}]	Diameter D_P [µm]	Provider
PMMA	1.190 ± 0.002	406.0 ± 9.5	Micro particles GmbH
Soda lime glass	2.530 ± 0.025	405.9 ± 8.7	Technical Glass Company
Steel	7.73 ± 0.02	400 ± 1	Nanoball GmbH
Tungsten-carbide/ Cobalt (94:6)	14.95 ± 0.03	400 ± 20	Goodfellow
Liquid material	**Density ρ_s [g cm^{-3}]**	**Viscosity μ [mPa]**	**Provider**
Silicone oil 10	0.935 ± 0.005	9.95 ± 0.3	Basildon Chemicals
Silicone oil 100	0.965 ± 0.005	103.00 ± 3.3	Basildon Chemicals

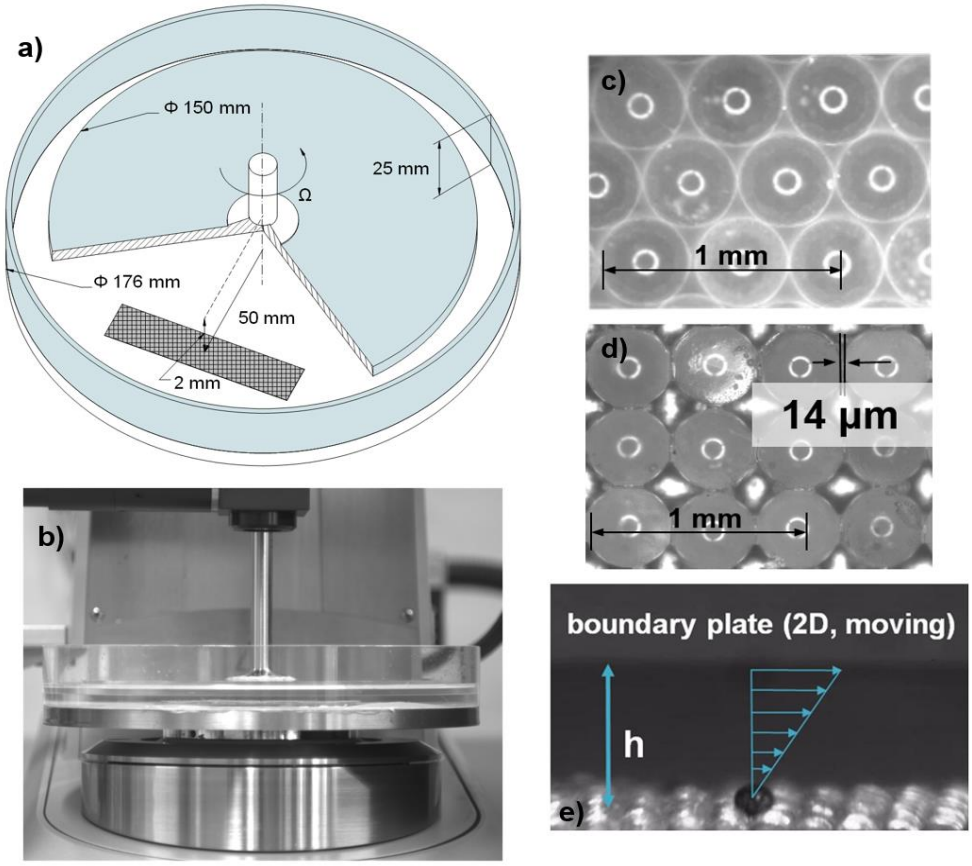

Fig.1: Sketch of the container and the rotating disk (a). Set-up including the container coupled to the rotational rheometer and the camera. Top view of regular substrates of identical spheres of (405.9 ± 8.7) µm diameter arranged according to triangular configuration (c) and quadratic configuration with a spacing of 14 µm between spheres (d). Lateral view of a particle placed on the quadratic substrate with a spacing of 14 µm (e).

Experimental results and discussion

We find a representative range of parameters independent from any boundary condition. We first check that the particle mean velocity is not affected by the rotating disk motion typical of our experimental set-up. According to previous studies, the critical Shields number for the onset of particle motion is hardly affected by the angle between the flow direction and the symmetrical axis of the substrate around its minimum values in an interval of about π/6 (Agudo and Wierschem 2012). Therefore, at a radius of 50 mm, the free bead should follows a straight path within around 17 mm with a very small interference from the rotating disk motion. This corresponds to about 30 positions for the quadratic substrate with wider spacing, i.e. the worst case.

Figure 2a represents the path followed by a glass particle on the quadratic substrate with narrow spacing, submitted to a Shields number that multiplies 2.5 times the critical value for the incipient motion. The initial position is in line to the symmetrical axis of the rotating disk at a radius of 50 mm from the center of the disk. The less viscous oil is used in this experiment to study the highest Particle Reynolds number case. The particle position is tracked from the top view during its displacement along 7 positions on the substrate. The distance is measured using a 1 mm stage micrometer and corresponds to a pathway of 2.99 ± 0.05 mm. Note that this distance is well below the critical distance beyond which the angle between flow direction and symmetrical axis start affecting the particle motion. As shown in Figure 2, the particle follows a completely straight-line motion. Only small fluctuations due to small irregularities on the substrate are observed.

Figure 2b shows the glass bead position in the stream-wise direction as a function of time for the quadratic substrate with narrow spacing. The less viscous oil is used again. The free bead is again submitted to Shields number of 0.1, i.e. at a value of 2.5 times the critical conditions. Results in diagram (b) are obtained from placing the free bead at the same radius, i.e. 50 mm, but displacing its initial positions from the symmetrical axis in the stream-wise direction (see inset in Figure 2b). The particle position, however, is tracked along the same region, i.e. 7 positions on the substrate starting from the position in line with the disk symmetrical axis, which corresponds to the distance of 2.99 ± 0.05 mm. The experiments are repeated two times. All the results collapse very well showing a linear dependence of the x-position with time (R2>0.9), independent from the initial position and from inertia for the considered particle Reynolds number. This demonstrates that the bead reaches the mean equilibrium velocity in an early stage (Agudo and Wierschem 2012). Apparently, there is no acceleration of the bead, which as expected, follows a linear trajectory along the 7 positions on the substrate. For the following studies, we always placed the particle at a radius of 50 mm from the center of the disk and we use a bead pathway of around 3 mm in order to calculate the mean particle velocity.

We also study the effect of small irregularities on the substrate surface on the main particle velocity. Figure 3 represents again the bead x-position as a function of time but for different pathways on the substrate at θ/θc = 1.3 (a) and θ/θc = 2.5 (b). Three different pathways situated one after other in the radial position are considered (see inset). All particle trajectories coincide within the range of uncertainty, being apparently local irregularities on the substrate negligible for measuring the mean velocity at this conditions. Note that the critical Shields number was first measured for all the local positions of the different pathways, showing values which agree with those obtained in previous studies within the range of uncertainty (Agudo and Wierschem 2012, Agudo *et. al* 2014). Also note that, at radius of 50 mm, variations on the radius of the order of around 0.5 mm are negligible as compared to other error sources.

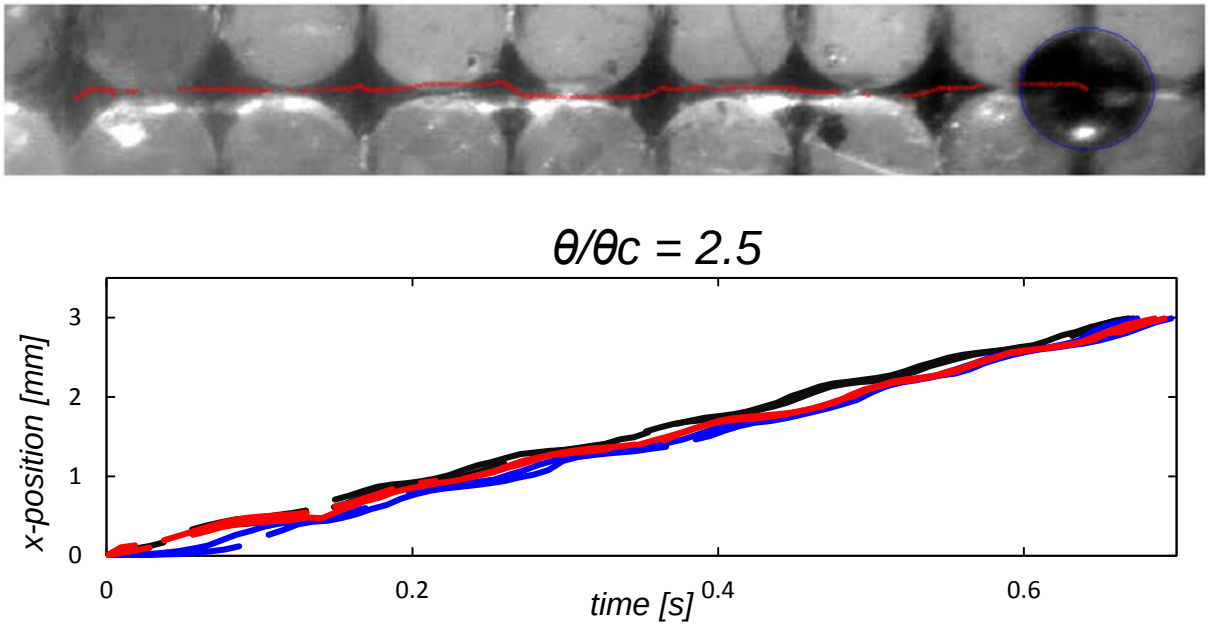

Fig. 2: Straight-line path experimented by a glass particle during its displacement along 7 positions on the quadratic substrate with a spacing of 14 μm between spheres (a). Particle x-position as a function of time during this displacement (b). Black, red and blue curves represent experiments with the particle placed on the initial position 0, -4 and -8, respectively. The experiments are performed using the less viscous oil at a radius of 50 mm and at constant Shields number of 0.1.

For Shields number only slightly higher than critical conditions (see Figure 3a), local deviations on the substrate structure apparently implies higher variation on the local velocity for different substrate pathways. The bead x-position describes a smooth repetitive oscillation with time which can be considered as a sinusoidal function. The amplitude remains constant and independent from the pathway, but we observe a small phase shift as a consequence of irregularities on the local substrate structure. Deviations on the main particle velocity for different pathways, however, are also of the same order of magnitude that the range of uncertainty for this case.

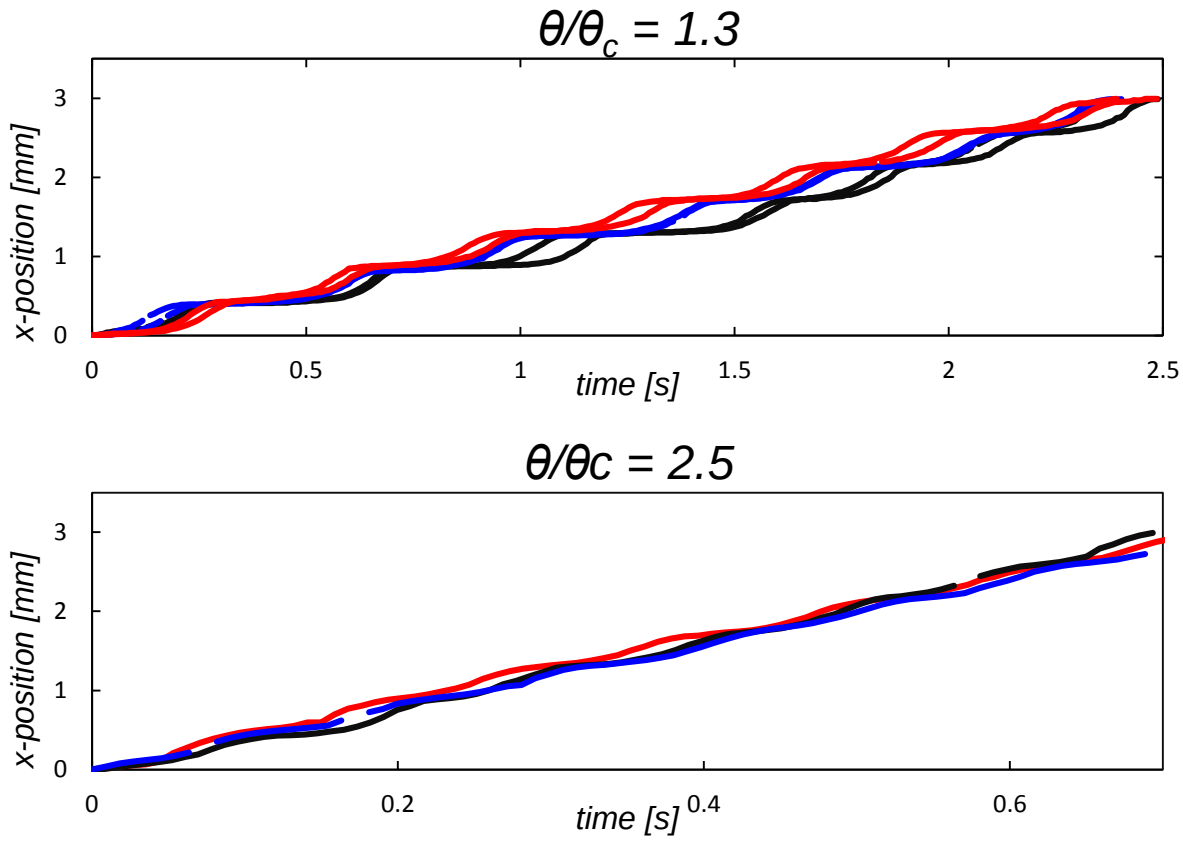

Fig. 3: Particle x-position as a function of time during its displacement along 7 positions on the quadratic substrate with a spacing of 14 μm between spheres at Shields numbers of 0.052 (a) and 0.1 (b). Black, red and blue curves represent experiments with the particle placed on the pathway 1, 2 and 3, respectively. The experiments are performed using the less viscous oil at a radius of 50 mm.

Summary

We study the influence of the substrate geometry on the particle main velocity using a rheometer working in a parallel-disk configuration. In order to check if the set-up is suitable for this purpose, we first find a representative range of parameters independent from any boundary conditions. In this way, it was observed that the particle experiments a completely straight-line motion during about 7 positions, i.e. around 3 mm on the quadratic substrate with narrow spacing at a radius of 50 mm. This distance is well enough for measuring a representative mean particle velocity. The moving particle reaches the mean equilibrium velocity in a very early stage of its displacement, independent from the initial position and from inertia for the considered particle Reynolds number. Furthermore, the particle mean velocity resulted independent from the followed pathway at a radius of around 50 mm, showing that the local irregularities of the substrate are negligible for measuring the experimental mean velocity on the set-up.

Acknowledgements

The authors are thankful to Mr. S. Schindler and Ms. E. Ojeda for collaborating in setting up the experiment. The support from Deutsche Forschungsgemeinschaft through WI 2672/4-1 is gratefully acknowledged.

References

Agudo, J.R., Wierschem, A., 2012: “Incipient motion of a single particle on regular substrates in laminar shear flow“, Phys. Fluids, 24, 093302

Agudo, J.R., Dasiva, S., Wierschem, A., 2014: “How do neighbors affect incipient particle motion in laminar shear flow?”, Phys. Fluids, 26, 053303

Charru, F., Larrieu, E., Dupont, J.-B., Zenit, R., 2007: “Motion of a particle near a rough wall in a viscous shear flow”, J. Fluid Mech., 570, pp. 431-453

Dey, S., Papanicolaou, A., 2008: “Sediment Threshold under Stream Flow: A State-of-the-Art Review”, KSCE J. Civ. Engng., 12, pp. 45-60

Derksen, J. J., 2011: “Simulations of granular bed erosion due to laminar shear flow near the critical Shields number”, Phys. Fluids 23, 113303

Groh, C., Wierschem, A., Aksel, N., Rehberg, I., Kruelle, C. A., 2008: “Barchan dunes in two dimensions: experimental tests of minimal models”, Phys. Rev. E 78, 021304

Lobkovsky, A. E., Orpe, A. V., Molloy, R., Kudrolli. Rothman, D. H., 2008: “Erosion of a granular bed driven by laminar fluid flow”, J. Fluid Mech. 605, pp. 47

Loiseleux, T., Gondret, P., Rabaud, M., Doppler, D., 2005: “Onset of erosion and avalanches for an inclined granular bed sheared by a continuous laminar flow”, Phys. Fluids 17, 103304

Ouriemi, M., Aussillous, P., Medale, M., Peysson, Y., Guazzelli, E., 2007: “Determination of the critical Shields number for particle erosion in laminar flow”, Phys. Fluids, 19, 061706

Pozo-Morales, L., Franco, M., Garvi, D., Lebrato, J., 2013: “Influence of the stone organization to avoid clogging in horizontal subsurface-flow treatment wetlands”, Ecol. Engineering, 54, pp. 136-144

Thompson, J. A., Bau, H. H., 2010: “Microfluidic, bead-based assay: Theory and experiments”, J. Chromatogr. B 878, pp 228

Swetzki, T., Rahmouni, S., Bechinger, C., Marr, D. W. M., 2008: “In situ assembly of linked geometrically coupled microdevices”, Proc. Natl. Acad. Sci. 105, 20141

Shields A., 1936: “Anwendungen der Aehnlichkeitsmechanik und der Turbulenzforschung auf die Geschiebebewegung”, Mitteilungen der Preußischen Versuchsanstalt für Wasserbau und Schiffbau ,26, pp. 1-26

Wierschem, A., Groh, C., Rehberg, I., Aksel, N., Kruelle C. A., 2008: “Ripple formation in weakly turbulent flow”, European Physical Journal, E 25, pp. 213-221

Wierschem, A., Groh, C., Rehberg, I., Aksel, N., Kruelle C. A., 2009: “Materialtransport bei der Rippelbildung in granularen Medien”, Proceeding of Lasermethoden in der Strömungsmesstechnik, 17. Fachtagung 2009, eds: A. Delgado, C. Rauh, H. Lienhart, B. Ruck, A. Leder, D. Dopheide, Erlangen, pp. 33.1 – 33.7

Wu, F. C., Chou, Y. J., 2003: “Rolling and Lifting Probabilities for Sediment Entrainment," J. Hydraul. Eng. 129, pp 2